

Ab initio nuclear physics from the Lattice Effective Field Theory

Bing-Nan Lü
呂炳楠

Nuclear Lattice EFT Collaboration



中国工程物理研究院研究生院
GRADUATE SCHOOL OF CHINA ACADEMY OF ENGINEERING PHYSICS



MICHIGAN STATE
UNIVERSITY



中山大學
SUN YAT-SEN UNIVERSITY



OAK RIDGE
National Laboratory
LEADERSHIP COMPUTING FACILITY

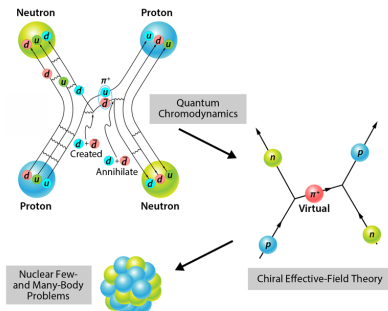


Hangzhou Institute for Advanced Study, UCAS, Hang-Zhou, May-18-2024

Chiral effective field theory

Chiral EFT: The low-energy equivalence of the QCD
Weinberg (1979,1990,1991), Gasser, Leutwyler (1984,1985)

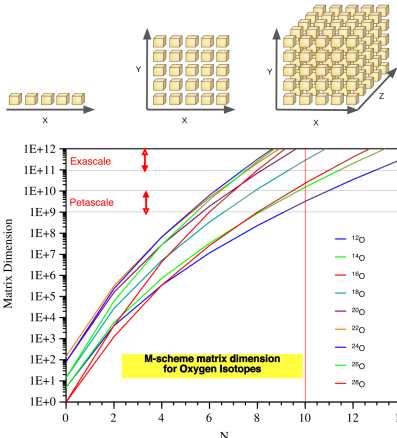
- Proton (uud), neutron (udd), pion ($u\bar{d}$)
- Spontaneously broken chiral symmetry:
 $SU(2)_L \times SU(2)_R \rightarrow SU(2)_V$
- Goldstone theorem implies a light pion:
Long-range part of the nuclear force
- Contact terms:
Short-range part of the nuclear force
- Hard scale: $\Lambda_\chi \sim 1 \text{ GeV}$: Chiral EFT works for momentum $Q \ll \Lambda_\chi$



Quarks confined
in nucleons and pions

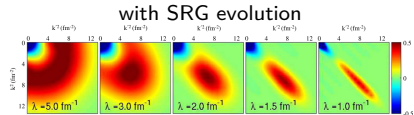
Dimensionality curse in nuclear many-body problems

Exponential increase of resources



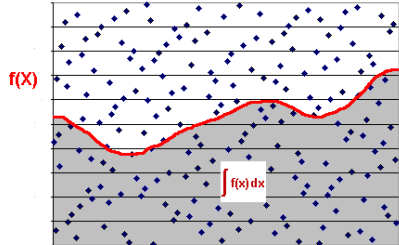
PRC 101, 014318 (2020)

Solution 1: Reduce effective Hilbert space



Solution 2: Monte Carlo algorithms

The Monte Carlo Integral

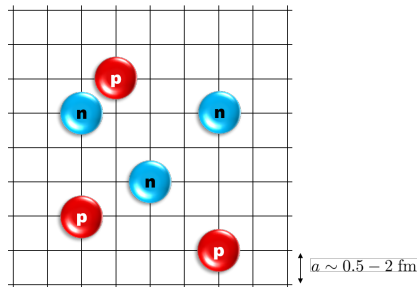


Introduction to Lattice Effective Field Theory

Lattice EFT = Chiral EFT + Lattice + Monte Carlo

Review: Dean Lee, Prog. Part. Nucl. Phys. 63, 117 (2009),
Lähde, Meißner, "Nuclear Lattice Effective Field Theory", Springer (2019)

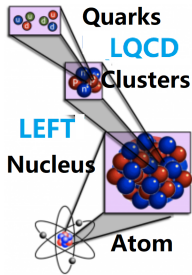
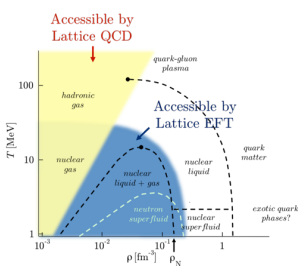
- Discretized **chiral nuclear force**
- Lattice spacing $a \approx 1 \text{ fm} = 620 \text{ MeV}$
(\sim chiral symmetry breaking scale)
- Protons & neutrons interacting via
short-range, δ -like and **long-range,**
pion-exchange interactions
- Exact method, **polynomial scaling** ($\sim A^2$)



Lattice adapted for nucleus

Comparison to Lattice QCD

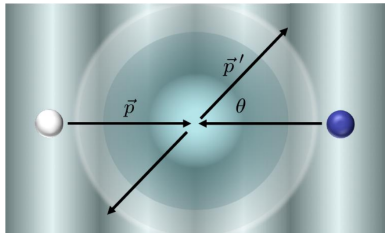
	LQCD	LEFT
degree of freedom	quarks & gluons	nucleons and pions
lattice spacing	$\sim 0.1 \text{ fm}$	$\sim 1 \text{ fm}$
dispersion relation	relativistic	non-relativistic
renormalizability	renormalizable	effective field theory
continuum limit	yes	no
Coulomb	difficult	easy
accessibility	high T / low ρ	low T / ρ_{sat}
sign problem	severe for $\mu > 0$	moderate



N-N scattering in the center of mass frame

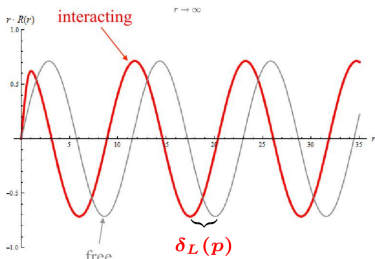
For scattering in the **continuum**:

- Partial wave expansion:
 $\psi(\vec{r}) = \sum_{J=0}^{\infty} \psi_J(r) P_J(\cos \theta)$
- Asymptotically ($r > R_{\text{force}}$):
 $\psi_J(r) \rightarrow A h_J^+(kr) - B h_J^-(kr)$
- Phase shift: $e^{2i\delta} = B/A$



For scattering in a **finite volume**:

- Luescher's formula:
$$e^{2i\delta} = \frac{Z_{00}(1;q^2) + i\pi^{3/2}q}{Z_{00}(1;q^2) - i\pi^{3/2}q}, \quad q = \frac{2\pi n}{L}$$
$$Z_{00}(s, q^2) = \frac{1}{\sqrt{4\pi}} \sum_n \frac{1}{(n^2 - q^2)^s}$$
- Standard tool in LQCD
[Beane et al., Int. J. Mod. Phys. E 17\(2008\) 1517](#)
- Not applicable in LEFT: noisy data, need higher precision



N - N interaction in nuclear chiral EFT

$$\langle \mathbf{p}'_1, \mathbf{p}'_2 | V_{N-N} | \mathbf{p}_1, \mathbf{p}_2 \rangle = \left\{ B_1 + B_2(\boldsymbol{\sigma}_1 \cdot \boldsymbol{\sigma}_2) + C_1 q^2 + C_2 q^2 (\boldsymbol{\tau}_1 \cdot \boldsymbol{\tau}_2) + C_3 q^2 (\boldsymbol{\sigma}_1 \cdot \boldsymbol{\sigma}_2) + C_4 q^2 (\boldsymbol{\sigma}_1 \cdot \boldsymbol{\sigma}_2)(\boldsymbol{\tau}_1 \cdot \boldsymbol{\tau}_2) \right. \\ + C_5 \frac{i}{2} (\mathbf{q} \times \mathbf{k}) \cdot (\boldsymbol{\sigma}_1 + \boldsymbol{\sigma}_2) + C_6 (\boldsymbol{\sigma}_1 \cdot \mathbf{q})(\boldsymbol{\sigma}_2 \cdot \mathbf{q}) + C_7 (\boldsymbol{\sigma}_1 \cdot \mathbf{q})(\boldsymbol{\sigma}_2 \cdot \mathbf{q})(\boldsymbol{\tau}_1 \cdot \boldsymbol{\tau}_2) \\ \left. - \frac{g_A^2}{4F_\pi^2} \left[\frac{(\boldsymbol{\sigma}_1 \cdot \mathbf{q})(\boldsymbol{\sigma}_2 \cdot \mathbf{q})}{q^2 + M_\pi^2} + C_\pi \boldsymbol{\sigma}_1 \cdot \boldsymbol{\sigma}_2 \right] (\boldsymbol{\tau}_1 \cdot \boldsymbol{\tau}_2) + \dots \right\} \delta(\mathbf{p}_1 + \mathbf{p}_2 - \mathbf{p}'_1 - \mathbf{p}'_2),$$

$\mathbf{q} = \mathbf{p}'_1 - \mathbf{p}_1, \mathbf{k} = \mathbf{p}'_2 - \mathbf{p}_2, \boldsymbol{\sigma}_{1,2}$ for spins, $\boldsymbol{\tau}_{1,2}$ for isospins, C_{1-7} , g_A , etc. are Low Energy Constants fitted to N - N scattering data

	Two-nucleon force	Three-nucleon force	Four-nucleon force
$\mathcal{O}((Q/\Lambda_\chi)^0)$	X H	—	—
	2 LECs		
$\mathcal{O}((Q/\Lambda_\chi)^2)$	X e K H	—	—
	7 LECs		
$\mathcal{O}((Q/\Lambda_\chi)^3)$	H K	X X *	—
	2 LECs		
$\mathcal{O}((Q/\Lambda_\chi)^4)$	X e K H ...	K H K X ...	H H H H ...
	15 LECs		

Euclidean time projection

- Get interacting g. s. from imaginary time projection:

$$|\Psi_{g.s.}\rangle \propto \lim_{\tau \rightarrow \infty} \exp(-\tau H) |\Psi_A\rangle$$

with $|\Psi_A\rangle$ representing A free nucleons.

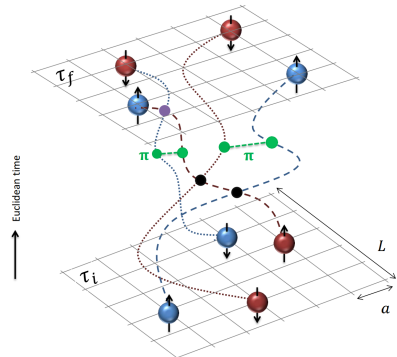
- Expectation value of any operator \mathcal{O} :

$$\langle \mathcal{O} \rangle = \lim_{\tau \rightarrow \infty} \frac{\langle \Psi_A | \exp(-\tau H/2) \mathcal{O} \exp(-\tau H/2) | \Psi_A \rangle}{\langle \Psi_A | \exp(-\tau H) | \Psi_A \rangle}$$

- τ is discretized into time slices:

$$\exp(-\tau H) \simeq \left[: \exp\left(-\frac{\tau}{L_t} H\right) : \right]^{L_t}$$

All possible configurations in $\tau \in [\tau_i, \tau_f]$ are sampled.
Complex structures like nucleon clustering emerges naturally.

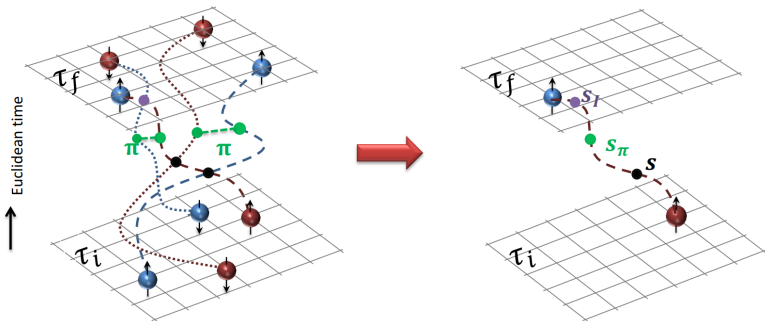


Auxiliary field transformation

- Quantum correlations between nucleons are represented by fluctuations of the auxiliary fields.

$$:\exp\left[-\frac{a_t C}{2}(\psi^\dagger \psi)^2\right] := \frac{1}{\sqrt{2\pi}} \int ds : \exp\left[-\frac{s^2}{2} + \sqrt{-a_t C} s (\psi^\dagger \psi)\right] :$$

- Long-range interactions such as OPEP or more complex interactions can be represented similarly.
- For fixed aux. fields, product of s.p. states (e.g., Slater determinant) keep the form of product of s.p. states in propagations. \Leftarrow **No N-N interaction**



Preparation of trial states

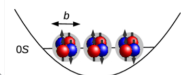
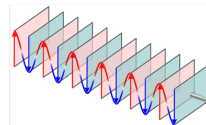
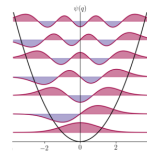
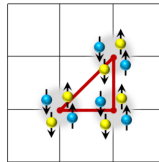
- Trial state can be chosen arbitrarily as long as its overlap with real ground state is large.

- A convenient choice is Slater determinant

$$|\Psi\rangle = \begin{vmatrix} \psi_1(\mathbf{r}_1) & \psi_1(\mathbf{r}_2) & \cdots & \psi_1(\mathbf{r}_A) \\ \psi_2(\mathbf{r}_1) & \psi_2(\mathbf{r}_2) & \cdots & \psi_2(\mathbf{r}_A) \\ \vdots & \vdots & \ddots & \vdots \\ \psi_A(\mathbf{r}_1) & \psi_A(\mathbf{r}_2) & \cdots & \psi_A(\mathbf{r}_A) \end{vmatrix}$$

- The single-particle wave functions can be either

- Gaussian wave packets
- Shell model wave functions
- Plane waves
- Alpha cluster wave functions



Evolution of Slater determinants

In imaginary time evolution, each s.p. wave function evolves independently

$$M(s_{n_t})(\psi_1 \wedge \psi_2 \wedge \cdots \wedge \psi_A) = M(s_{n_t})\psi_1 \wedge M(s_{n_t})\psi_2 \wedge \cdots \wedge M(s_{n_t})\psi_A,$$

because there is no direct interactions between nucleons.

Monte Carlo integration technique

- We are interested in the ratio

$$\begin{aligned}\langle O \rangle &= \lim_{\tau \rightarrow \infty} \frac{\int \mathcal{D}s (\Psi_T | M(s_{L_t}) \cdots M(s_{L_t/2+1}) O M(s_{L_t/2}) \cdots M(s_1) | \Psi_T)}{\int \mathcal{D}s (\Psi_T | M(s_{L_t}) \cdots M(s_1) | \Psi_T)} = \lim_{\tau \rightarrow \infty} \frac{\int \mathcal{D}s \mathcal{M}_O(s)}{\int \mathcal{D}s \mathcal{M}(s)} \\ &= \lim_{\tau \rightarrow \infty} \frac{\int \mathcal{D}s |\mathcal{M}(s)| \frac{\mathcal{M}_O(s)}{|\mathcal{M}(s)|}}{\int \mathcal{D}s |\mathcal{M}(s)| \frac{\mathcal{M}(s)}{|\mathcal{M}(s)|}} = \lim_{\tau \rightarrow \infty} \frac{\langle \frac{\mathcal{M}_O(s)}{|\mathcal{M}(s)|} \rangle}{\langle \frac{\mathcal{M}(s)}{|\mathcal{M}(s)|} \rangle}\end{aligned}$$

In last step we rewrite the integral into an expectation value in a ensemble of s fields with probability distribution $P(s) \propto |\mathcal{M}(s)|$. Note that the overall normalization factors are always canceled.

- We need to generate the s fields with probability $P(s)$, this can be achieved with the Metropolis algorithm
 - For any fixe s , generate a random new configuration s'
 - Compute the ratio $\eta_{s \rightarrow s'} = \frac{P(s')}{P(s)} = \frac{|\mathcal{M}(s')|}{|\mathcal{M}(s)|}$
 - Choose a random number $r \in U(0,1)$
 - If $\eta_{s \rightarrow s'} > r$, accept; otherwise reject.
- Wait until the s -ensamble converge to the desired distribution $P(s) \propto |\mathcal{M}(s)|$.
- Choose N samples s_1, s_2, \dots, s_N in the s -ensamble, calculate $\mathcal{M}(s_k)$ and $\mathcal{M}_O(s_k)$ seperately. Then the expectation value can be estimated unbiasedly as

$$\langle O \rangle = \lim_{\tau \rightarrow \infty} \frac{\sum_k \mathcal{M}_O(s_k) / |\mathcal{M}(s_k)|}{\sum_k \mathcal{M}(s_k) / |\mathcal{M}(s_k)|},$$

with a statistical error scales as $\mathcal{O}(1/\sqrt{N})$.

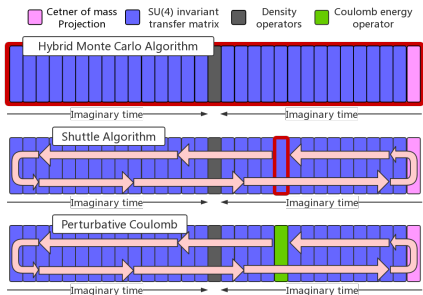
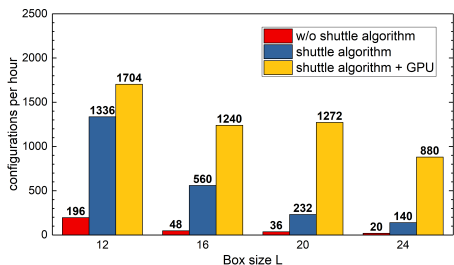
Advanced algorithm and programming paradigm

All $L_t \times L^3$ auxiliary fields s_{n,n_t} need to be updated. Two algorithms:

- Update all fields once every iteration: **Hybrid Monte Carlo**
- Update a single time slice every iteration: **Shuttle Algorithm**

B.L., et. al., PLB 797, 134863 (2019)

SA 5~10 times faster than HMC



- Can be implemented for GPU
- **Algorithm & Hardware** combined give a **40~50 times** speed-up

Large lattices are accessible

Essential elements of the nuclear force

We use a zeroth order lattice Hamiltonian that respects the Wigner-SU(4) symmetry

$$H_0 = K + \frac{1}{2} C_{\text{SU4}} \sum_{\mathbf{n}} : \tilde{\rho}^2(\mathbf{n}) :$$

The smeared density operator $\tilde{\rho}(\mathbf{n})$ is defined as

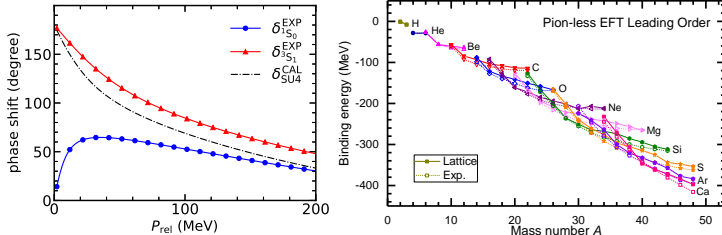
$$\tilde{\rho}(\mathbf{n}) = \sum_i \tilde{a}_i^\dagger(\mathbf{n}) \tilde{a}_i(\mathbf{n}) + s_L \sum_{|\mathbf{n}' - \mathbf{n}|=1} \sum_i \tilde{a}_i^\dagger(\mathbf{n}') \tilde{a}_i(\mathbf{n}'), \quad (1)$$

where i is the joint spin-isospin index

$$\tilde{a}_i(\mathbf{n}) = a_i(\mathbf{n}) + s_{NL} \sum_{|\mathbf{n}' - \mathbf{n}|=1} a_i(\mathbf{n}'). \quad (2)$$

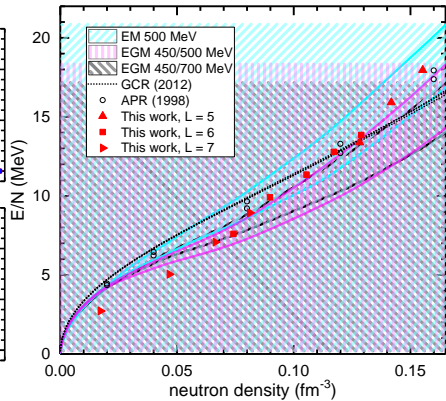
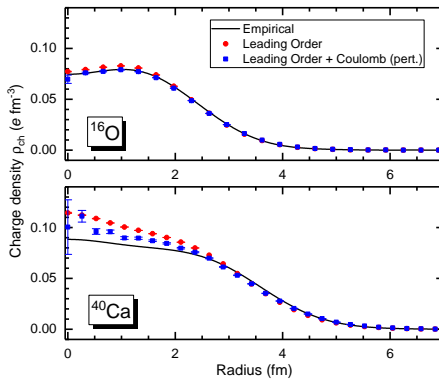
In this work we use a lattice spacing $a = 1.32$ fm and the parameter set

$$C_{\text{SU4}} = -3.41 \times 10^{-7} \text{ MeV}^{-2}, s_L = 0.061 \text{ and } s_{NL} = 0.5.$$



Essential elements for nuclear binding

Charge density and neutron matter equation of state
are important in element creation, neutron star merger, etc.



Lu et al., PLB 797, 134863 (2019)

Perturbative quantum Monte Carlo method

Table: The nuclear binding energies at different orders calculated with the ptQMC.
 E_{exp} is the experimental value. All energies are in MeV. We only show statistical errors from the MC simulations.

	E_0	δE_1	E_1	δE_2	E_2	E_{exp}
^3H	-7.41(3)	+2.08	-5.33(3)	-2.99	-8.32(3)	-8.48
^4He	-23.1(0)	-0.2	-23.3(0)	-5.8	-29.1(1)	-28.3
^8Be	-44.9(4)	-1.7	-46.6(4)	-11.1	-57.7(4)	-56.5
^{12}C	-68.3(4)	-1.8	-70.1(4)	-18.8	-88.9(3)	-92.2
^{16}O	-94.1(2)	-5.6	-99.7(2)	-29.7	-129.4(2)	-127.6
$^{16}\text{O}^\dagger$	-127.6(4)	+24.2	-103.4(4)	-24.3	-127.7(2)	-127.6
$^{16}\text{O}^\ddagger$	-161.5(1)	+56.8	-104.7(2)	-22.3	-127.0(2)	-127.6

Realistic N²LO chiral Hamiltonian fixed by few-body data + perturbative quantum MC simulation = nice agreement with the experiments

Excellent agreement \implies Demonstration of **nuclear force** & **many-body algorithm**

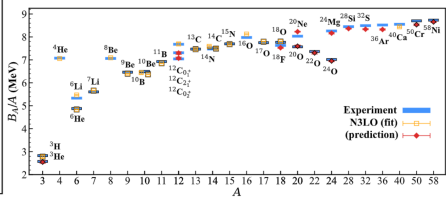
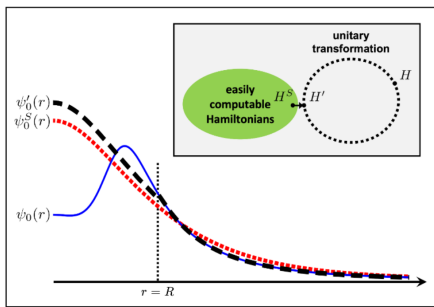
Also applicable for densities & matrix elements

Lu *et al.*, PRL 128, 242501 (2022)

Wave function matching method

Unitarily transformed Hamiltonian $H \rightarrow H' = UHU^\dagger$ reproduce the same **low-energy** (large-scale) physics

⇒ Design an operator U that H' is much easier to handle than H (e.g., H' with weaker sign problem in Monte Carlo)

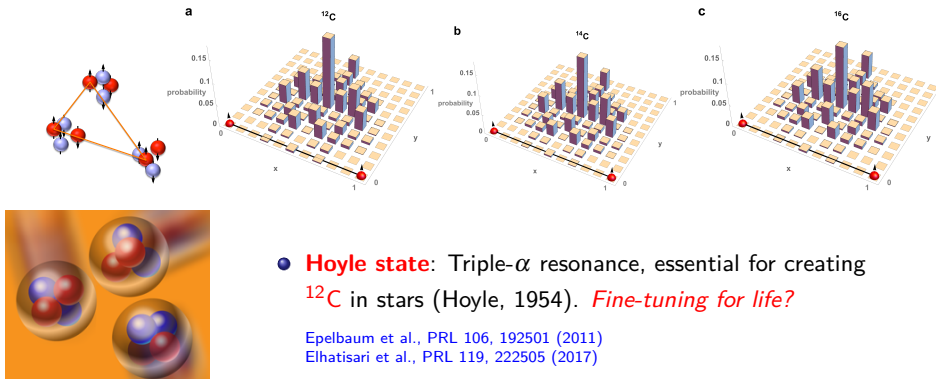


S. Elhatisari *et al.*, arXiv:2210.17488, accepted by Nature

Many-body correlations: α -cluster geometry in C isotopes

We always align the longest edge with the x -axis
and keep the triangle in the x - y plane.

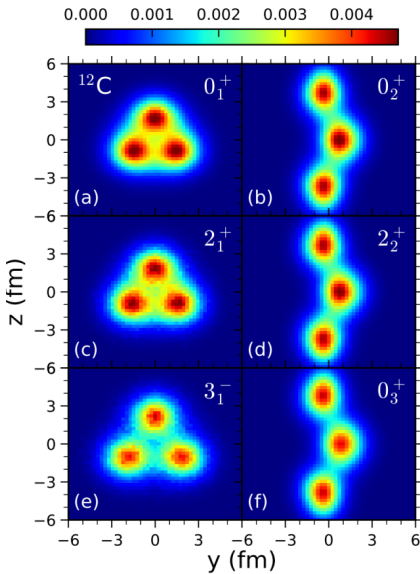
$$\rho(d_1, d_2, d_3) = \sum_{j_1 j_2 j_3} \sum_{\mathbf{n}_1, \mathbf{n}_2, \mathbf{n}_3} |\Phi_{\uparrow j_1, \uparrow j_2, \uparrow j_3}(\mathbf{n}_1, \mathbf{n}_2, \mathbf{n}_3)|^2 \\ \times \sum_{P(123)} \delta(|\mathbf{n}_1 - \mathbf{n}_2| - d_3) \delta(|\mathbf{n}_1 - \mathbf{n}_3| - d_2) \delta(|\mathbf{n}_2 - \mathbf{n}_3| - d_1),$$



- **Hoyle state:** Triple- α resonance, essential for creating ^{12}C in stars (Hoyle, 1954). *Fine-tuning for life?*

Epelbaum et al., PRL 106, 192501 (2011)
Elhatisari et al., PRL 119, 222505 (2017)

Clustering from first principle: Tomographic scan of ^{12}C

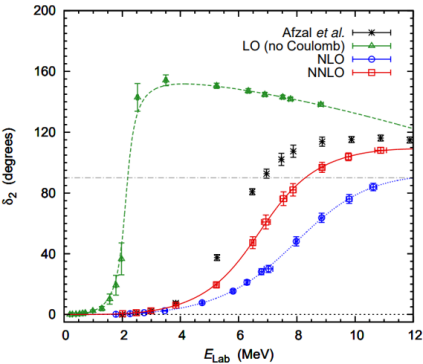
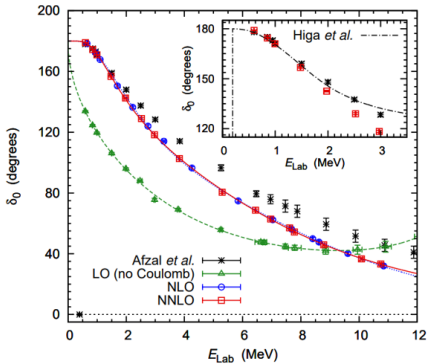


- Structure of ^{12}C states are full of complexity and duality (clustering v.s. mean-field)
- we provide the first model-independent tomographic scan of the three-dimensional geometry of the nuclear states of ^{12}C using the ab initio framework of nuclear lattice EFT.
- 0_1^+ : ground state, 0_2^+ : Hoyle state

Sihang Shen et al., Nat. Comm. 14, 2777 (2023)

α - α scattering from lattice EFT

Ab-initio alpha-alpha scattering N2LO

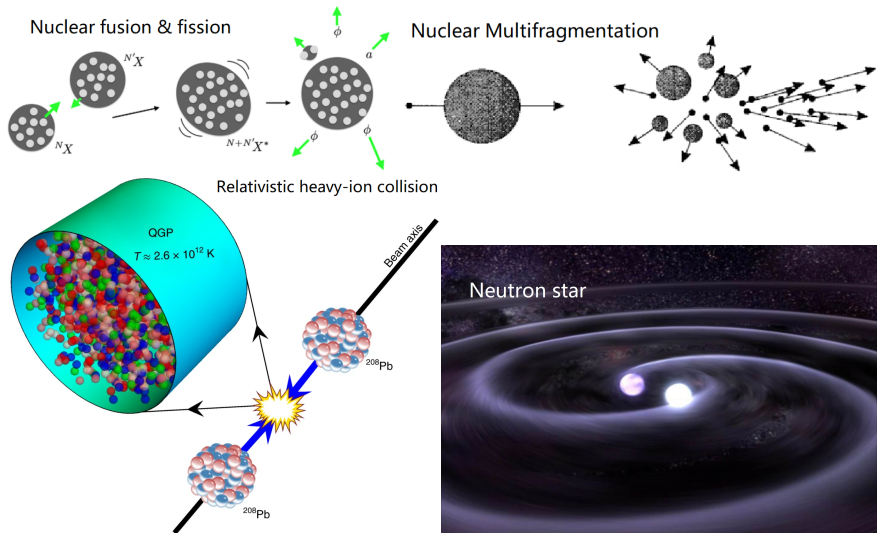


Afzal, Ahmad, Ali, *Rev. Mod. Phys.* 41, 247, (1969).

Higa, Hammer, van Kolck, *Nucl.Phys.* A809, 171 (2008), 0802.3426.

S.E., Lee, Rupak, Epelbaum, Krebs, Lähde, Luu, & Meißner. *Nature* 528, 111-114 (2015).

Hot nucleus with pinhole trace algorithm

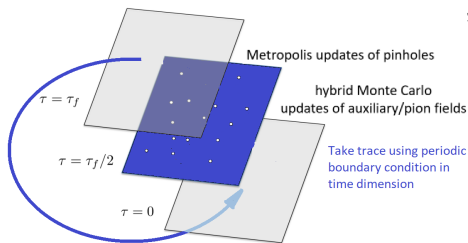


Simulate canonical ensemble with pinhole trace algorithm

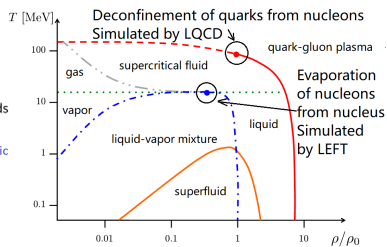
- All we need: **partition function** $Z(T, V, A) = \sum_k \langle \exp(-\beta H) \rangle_k$, sum over all orthonormal states in Hilbert space $\mathcal{H}(V, A)$.
- The **basis states** $|\mathbf{n}_1, \mathbf{n}_2, \dots, \mathbf{n}_A\rangle$ span the whole **A-body Hilbert space**.
 $\mathbf{n}_i = (\mathbf{r}_i, s_i \sigma_i)$ consists of **coordinate, spin, isospin** of i -th nucleon.
- **Canonical partition function** can be expressed in this **complete basis**:

$$Z_A = \text{Tr}_A [\exp(-\beta H)] = \sum_{\mathbf{n}_1, \dots, \mathbf{n}_A} \int \mathcal{D}s \mathcal{D}\pi \langle \mathbf{n}_1, \dots, \mathbf{n}_A | \exp[-\beta H(s, \pi)] | \mathbf{n}_1, \dots, \mathbf{n}_A \rangle$$

- **Pinhole algorithm** + **periodicity in β** = **Pinhole trace**
- Apply **twisted boundary condition** in 3 spatial dimensions to remove finite volume effects. Twist angle θ averaged with MC.



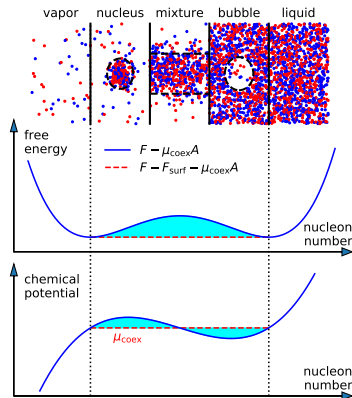
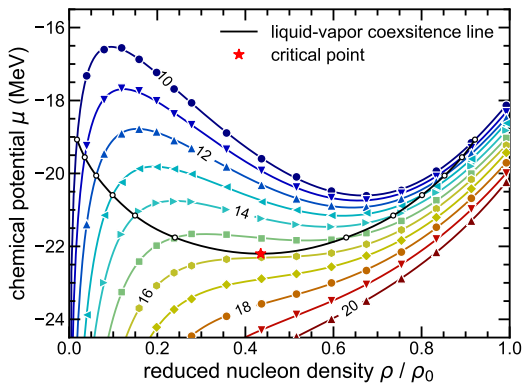
Lu et al., PRL 125, 192502 (2020)



Finite nuclear systems: Liquid-vapor coexistence line

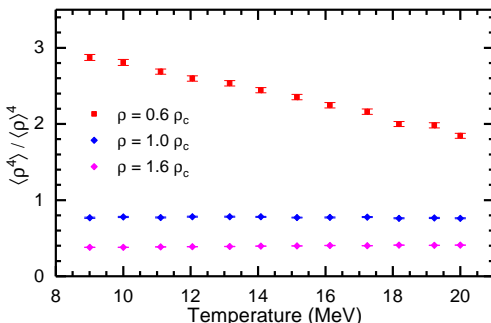
- First *ab initio* calculation of nuclear liquid-gas phase transition.
- Symmetric nuclear matter $N = Z$, lattice spacing $a = 1.32 \text{ fm}$, volume $V = (6a)^3$, nucleon number $4 \leq A \leq 132$.
- Temperature $10 \text{ MeV} \leq T \leq 20 \text{ MeV}$, temporal step $\Delta\beta = 1/2000 \text{ MeV}^{-1}$.
- 288000 independent measurements for every data point.

Lu et al., PRL 125, 192502 (2020)



Other observables: Clustering in hot nuclear matter

- Mean field models can yield **bulk properties**. However, microscopic observables like **clustering** play important role in experiments.
- Fisher's droplet model** see hot nucleus as a mixture of small droplets, F = volume term + surface terms, **not microscopic**.
- Ab initio** calculation unifies all calculations in a **single framework** with **microscopic foundations**.
- Test: Ratio $\langle \rho^4 \rangle / \langle \rho \rangle^4$ signifies the **clustering correlation**.



Lu et al., PRL 125, 192502 (2020)

Count clusters in hot nuclear matter

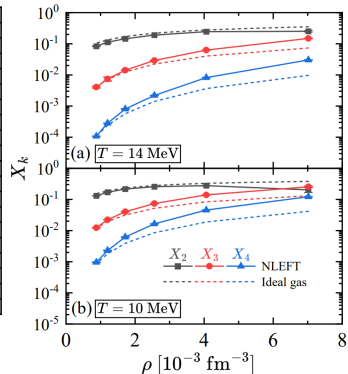
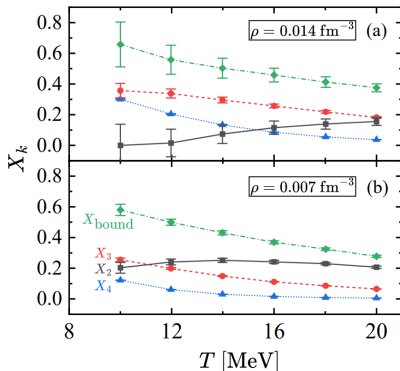
- By expanding the correlation functions on a basis of cluster correlation functions, the probability / mass fraction of clusters can be extracted

$$\langle G_{11}(n) \rangle = \langle G_{11}^l \rangle + w_4 \langle G_{11}(n) \rangle_4 + w_3 \langle G_{11}(n) \rangle_3 + w_2 \langle G_{11}(n) \rangle_2$$

$$\langle G_{21}(n) \rangle = \langle G_{21}^l \rangle + w_4 \langle G_{21}(n) \rangle_4 + w_3 \langle G_{21}(n) \rangle_3$$

$$\langle G_{31}(n) \rangle = \langle G_{31}^l \rangle + w_4 \langle G_{31}(n) \rangle_4$$

$$\langle G_{22}(n) \rangle = \langle G_{22}^l \rangle + w_4 \langle G_{22}(n) \rangle_4, \quad X_k = w_k k/A$$



"Ab initio study of nuclear clustering in hot dilute nuclear matter"
ZhengXue Ren et al., PLB 850, 138463 (2024)

Structure factors with realistic chiral interactions

- Structure factors are Fourier transforms of correlation functions

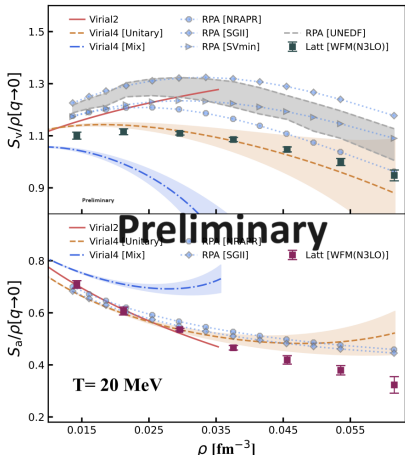
$$S_V(\mathbf{q}) = \int d^3r [\langle \hat{\rho}(\mathbf{r} + \mathbf{r}') \hat{\rho}(\mathbf{r}') \rangle - \rho_0^2] e^{-i\mathbf{q} \cdot \mathbf{r}}$$

$$S_a(\mathbf{q}) = \int d^3r [\hat{\rho}_z(\mathbf{r} + \mathbf{r}') \hat{\rho}_z(\mathbf{r}') \rangle - \rho_{z0}^2] e^{-i\mathbf{q} \cdot \mathbf{r}}$$

- Key for modeling Core-collapse supernovae explosions via neutrino-nucleon scattering

- Ab initio calculation with a N³LO chiral interaction based on a rank-one operator method

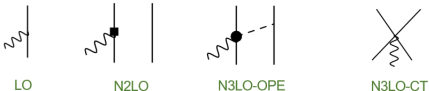
YuanZhuo Ma et al.,
arXiv:2306.04500, accepted by PRL



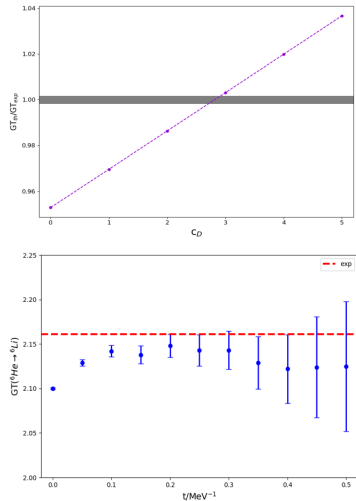
Exploring Nuclear β -decay Through NLEFT

Teng et al. in progress

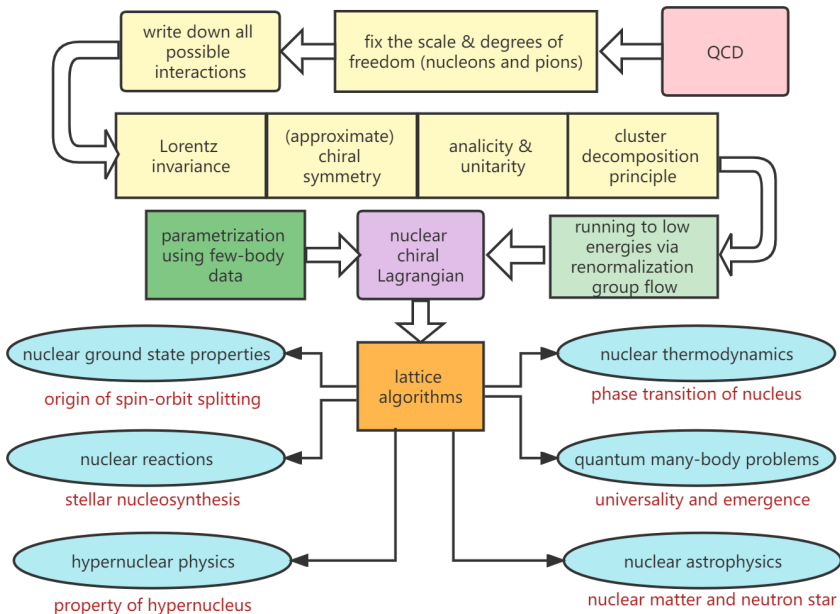
- ★ The first explorative study on nuclear β -decay via NLEFT.
- ★ N2LO chiral nuclear force + chiral axial current up to N3LO.



- ★ ^3H β -decay is studied to help determine 3N LECs.
- ★ Promising results on ^6He β -decay.



Summary



THANK YOU FOR YOUR
ATTENTION